Aqueous MAPA, DEEA and their blend as CO_2 absorbents: Interrelationship between NMR speciation, pH and heat of absorption data

Cristina Perinu,[1] Ida M. Bernhardsen,[2] Diego D.D. Pinto,[2] Hanna K. Knuutila,[2]

Klaus J. Jens.*[1]

[1]Department of Process, Energy and Environmental Technology, University of Southeast Norway, Postbox 235, NO-3603 Kongsberg, Norway

[2]Department of Chemical Engineering, Norwegian University of Science and Technology (NTNU), NO-7491 Trondheim, Norway

* klaus.j.jens@usn.no

ABSTRACT

Based on NMR speciation, heat of absorption and pH data, the reactions occurring in aqueous MAPA (3-(Methylamino)propylamine), DEEA (2-(Diethylamino)ethanol) and their blend at various carbon dioxide (CO_2) loadings were identified and discussed.

At increasing CO_2 loading, the basicity of the solutions decreased. In the MAPA solvent, this led to the hydrolysis of the carbamate species, which corresponded to a drop in the heat of absorption. In the blend, due to the activity of DEEA, such a drop in both pH and heat of absorption was not noticeable. In the presence of MAPA, in the early loadings DEEA had not

yet an influence on the (bi)carbonate formation, but mainly on the MAPA activity. However, as soon as the trend for (bi)carbonate formation went as in DEEA singly, the released heat steadily decreased. Both in single and blended MAPA, the carbamate hydrolyses started at similar pH values, i.e. about 9.8-9.5.

1. INTRODUCTION

1.1. Background

Carbon dioxide (CO_2) from human activities has been recognized as the greenhouse gas making the largest contribution to the global warming, and actions to reduce its concentration in the atmosphere are solicited. [1] Amine scrubbing is one of the most common technology for removal of CO_2 from flue, natural and other exhaust gases of different industrial sources.[2] The benchmark absorbent is monoethanolamine (MEA, a primary amine) in an aqueous mean, which is known for its high reactivity and favorable reaction kinetics toward CO_2, but it suffers from degradation and unfavorable thermodynamics.[3] Replacing MEA is a challenging task because the selection of any new absorbent should take into account several key criteria, like e.g. chemical and physical properties of the solvents, kinetics and thermodynamics of chemical reactions, environmental impacts, costs and so on.[4]

To reach ideal solvent properties, aqueous blended amines are receiving great attention, as the best features of two or more amines can be combined and/or even improved.[5] The mixture composed of MAPA, 3-(Methylamino)propylamine, and DEEA, 2-(Diethylamino)ethanol, is a promising CO_2 absorbent. MAPA is a diamine, composed of a primary and a secondary amino functional group, which shows favorable kinetics of reaction but high heat of absorption, while for DEEA, a tertiary amine, the opposite is true.[6] Several key properties, like e.g. heat of absorption, kinetics and volatility, of MAPA-DEEA blends both as single phase and/or as de-mixing solvent have been studied.[7-9] The reaction mechanisms of MAPA and DEEA, singly and in blend, is also under investigation as it would allow the optimization of the existing solvents and the design of new ones with improved properties. Recently, Zhang et al. [10] performed an NMR speciation analysis for CO_2 loaded aqueous MAPA and MEDA (*N*-Methylethylenediamine), two diamines with different chain lengths, to understand the competitive reactions between the intramolecular amino functional groups. Based on the

amount of each species as well as on the pH values at various addition of CO_2, three different stages of reactions were identified for each amine solvent. However, in that study, MAPA was investigated singly only. In 2018, Perinu et al.[11] performed by means of NMR spectroscopy a chemical speciation analysis on MAPA, eight tertiary amines (including DEEA) and their blends after CO_2 absorption (40 °C) and desorption (80 °C) tests in a screening apparatus. For each amine system, the speciation analyses were performed on a unique sample withdrawn after the absorption screening experiments, which terminated when the effluent reached 9.5 kPa partial pressure of CO_2.[12] Highlights on the role played by the tertiary amines in the presence of MAPA were reported and it was hypothesized that the tertiary amines, which act as Brønsted bases, contribute to reduce the protonation of MAPA species in favor of MAPA carbamate formation. A list of the probable reactions was included in the study, but it was possible neither to confirm them nor to define at which stage of the CO_2 addition they were occurring.

During the absorption of CO_2 by an amine system in an aqueous mean, several acid-base reactions are involved, and the species found at the equilibrium depend on the chemical reactions occurred, which in turn depend on the chemical properties of the amines and reaction conditions. Many factors may indeed influence the CO_2 absorption capacity of a solvent, like e.g. type of amines and chemical structure, concentrations, basicity (pH of the solution and pK_a of the amines), reaction energy and so on, and when selecting a solvent, the different features should be taken into consideration.[13] Moreover, when two or more amines are in mixture, the CO_2 loaded amine systems become more complicated as each amine group react differently and the ratio between the amines has an impact too.

The primary reactions between amines and CO_2 in water are mainly known and largely discussed in literature. As general, in an aqueous amine system in the presence of CO_2, amine

1   carbamate ($R_1R_2NCOO^-$) and bicarbonate/carbonate (HCO_3^-/CO_3^{2-}) are the two main reaction

2   products, which strongly affects the total amount of CO_2 absorbed and released.

3   Amine carbamates are usually formed by the reaction of primary and/or secondary amines with

4   CO_2 in the presence of a base (Reaction 1).

5    $R_1R_2NH + CO_2 + B \leftrightarrows R_1R_2NCOO^- + BH^+$ (1)
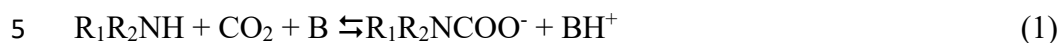
6   The base (B) can be an amine and/or water. The carbamate forming reaction is the reaction of

7   the lone pair of the amine nitrogen (which is a Lewis base) with the electrophilic centre (Lewis

8   acid) of CO_2.[14] Several mechanisms have been proposed in literature (Scheme 1) and, due to

9   the fast kinetics and the wide range of amine conditions (such as type of amine, concentrations,

10   pK_a), they are still under debate.[15, 16] One possibility is that the amine carbamate is formed

11   through an intermediate, either carbamic acid (Scheme 1a)[16] or zwitterion (Scheme 1b)[17], or

12   through a single step (Scheme 1c)[18], that is a termolecular reaction between CO_2, the amine

13   and a base (B).

14

15
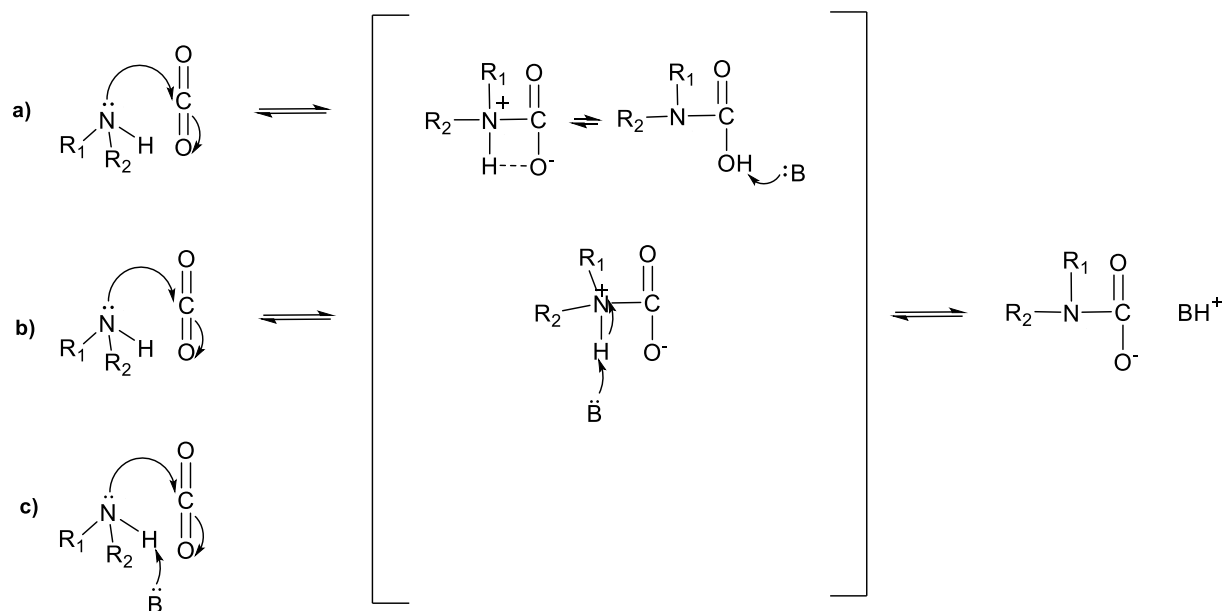
16   **Scheme 1.** The main reactions mechanisms available in literature for amine carbamate

17   formation. B represents a Brønsted base.

Secondary amines form amine carbamates less stable than those obtained by primary amines. The carbamate hydrolysis constants of secondary amines are at least one order of magnitude larger than those of corresponding primary amines.[19] This lower stability may be because the nitrogen (N-) atom is more hindered than in a primary amino group.

Tertiary amines cannot react with CO_2 directly, although a limited number of authors have observed the formation of alkyl carbonate in aqueous tertiary alkanolamines.[11, 20-23] Jørgensen and Faurholt[20] suggested the reaction (2) in basic aqueous solutions of amino alcohols, and proposed the overall reaction (3) (which represents the inverse of the alkyl carbonate hydrolysis) as they observed the formation of the alkyl carbonate when mixing amines, bicarbonate and carbonate.

$$R_1R_2N(CH_2)_nOH + CO_2 + OH^- \leftrightarrows R_1R_2N(CH_2)_nOCOO^- + H_2O \qquad (2)$$
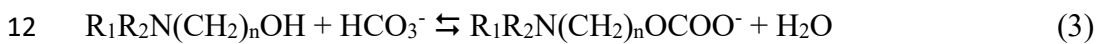
$$R_1R_2N(CH_2)_nOH + HCO_3^- \leftrightarrows R_1R_2N(CH_2)_nOCOO^- + H_2O \qquad (3)$$

At pH lower than 12, the rate of its formation is negligible and doesn't lead to relevant amount at equilibrium. However, the amount of this species is documented to increase at increasing CO_2 loading (decreasing pH), as reported in Beherens et al.[21] in a study specific on monolakylacarbonate formation in aqueous MDEA (Methyldiethanolamine). In that study, it was concluded that, though formed in relatively small amount and very little knowledge are available on it, those species must be taken into consideration in the models describing the liquid phase reactions. In most cases, this species was indeed neglected, and in some NMR studies the corresponding peaks were attributed to undefined side-products and/or impurities.

A primary reaction between CO_2 and tertiary amines in aqueous solutions is instead a kind of base catalysis of the CO_2 hydration leading to the formation of bicarbonate (reaction 4), through an acid-base buffer mechanism.

$$R_3N + CO_2 + H_2O \leftrightarrows R_3NH^+ + HCO_3^- \qquad (4)$$
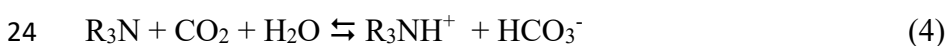
1   It is known that, in an aqueous mean, CO_2 can react with OH^- (reaction 5), followed by the

2   reaction 6, and H_2O (reaction 7).[24] Reaction 7 is negligible at pH higher than 10, whereas at

3   pH between 10 and 8 both reaction pathways (5 and 7) are possible.[25, 26] It is observed that the

4   loss of the proton from the H_2O molecules can cause an enormous increase in the affinity for

5   CO_2[27] and, then, the reaction 7 can be catalysed by chemical constituents able to get hydrogen

6   ions. On this regard, tertiary amines are good Brønsted bases, which by definition are

7   substances able to accept a proton (reaction 8). [24, 28] The pair of unshared electrons on the

8   nitrogen indeed enables amines to act as general base catalysts.

9    $CO_2 + OH^- \leftrightarrows HCO_3^-$ $\hspace{8cm}$ (5)

10   $HCO_3^- + OH^- \leftrightarrows CO_3^{2-} + H_2O$ $\hspace{6.5cm}$ (6)

11   $CO_2 + H_2O \leftrightarrows H_2CO_3 \leftrightarrows HCO_3^- + H^+$ $\hspace{5.5cm}$ (7)

12   $R_3N + H_2O \leftrightarrows R_3NH^+ + OH^-$ $\hspace{6.5cm}$ (8)

13   In literature, for (bi)carbonate formation in the presence of a tertiary amine, several

14   mechanisms have been proposed,[28] and for all of them the overall pathway is represented by

15   reaction 4 (overall reaction, 5+8). [22, 28, 29] A possible chemical path for reaction (4) is assumed

16   to be a termolecular reaction (scheme 2a) where a hydrogen bonding between the free amine

17   and water increases the nucleophilic reactivity of the water towards CO_2.[30, 31] Depending on

18   the basicity of the amines, a two-step cascade reaction is also possible, that is reaction 8

19   followed by reaction 5.[32] Moreover, it was also suggested the formation of an intermediate in

20   the catalytic path, as shown in the Scheme 2b.[28]

a)   b)
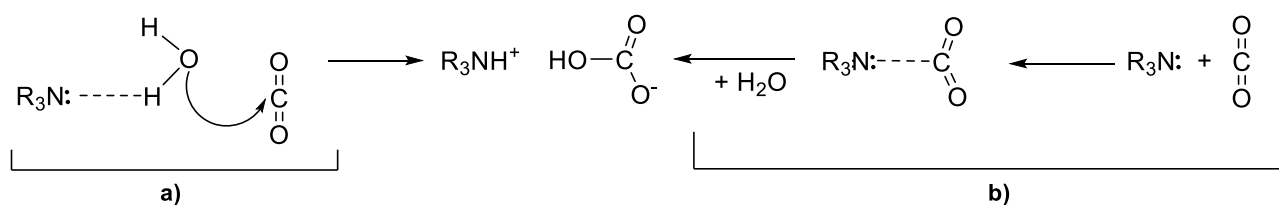
21

22   **Scheme 2.** Possible reaction mechanisms for CO_2 hydration catalyzed by a tertiary amine.

In addition, bicarbonate is also formed through the hydrolysis of the amine carbamate. Due to steric hindrance or weakly alkalinity, the amine carbamate can become unstable, leading to the formation of HCO_3^-, as in reaction 9.[33, 34]

$$R_1R_2NCOO^- + H_2O\ (+\ H^+) \leftrightharpoons R_1R_2NH(H^+) + HCO_3^- \qquad\qquad (9)$$
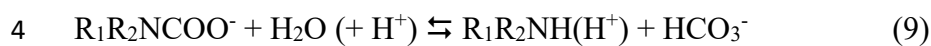
1.2. Aim of the work

An aqueous amine system in the presence of water and CO_2 leads to the occurrence of several parallel and/or consecutive reversible reactions. Knowing the structure and the amount of the reaction products is fundamental, as well as the measurement of the pH may be valuable to understand the dynamics leading to specific reaction pathways and the position of the acid-base reaction equilibria. By measuring pH, the status of equilibrium of all acid-base containing reactions is indeed measured. Moreover, the heat released during the addition of CO_2 in an amine solution is directly related to the steam consumption and gives information on how sensitive the system is when subject to a change in temperature.[35] The heat of absorption is given by the combination of the heat of physical dissolution of CO_2 into the amine solvent and the heat of reaction between CO_2 and the amine solvent. The formation of carbamate is an exothermic reaction, whose released heat is higher than that for the formation of bicarbonate.[7] The present study aims to understand the reaction mechanisms of the absorption of CO_2 in aqueous MAPA and DEEA, singly and in mixture, and the factors influencing them. Speciation analyses, as given by NMR (Nuclear Magnetic Resonance) spectroscopy, pH and heat of absorption measurements were performed at various addition of CO_2 in the amine solvents. The heat of absorption and pH measurements were combined to the NMR speciation data to be able to explain them in a more fundamental level. Insights on the chemical reactions are given, and reactions mechanisms are discussed.

2. EXPERIMENTAL SECTION

2.1 Chemicals

The chemicals 3-(Methylamino)propylamine (≥97%, CAS: 6291-84-5) and 2-(Diethylamino)ethanol (≥99.5%, CAS: 100-37-8) were purchased from Sigma-Aldrich, and Carbon Dioxide (99.999%) was purchased from AGA. The chemicals were used without further purification.

2.2 Sample preparation and density

Aqueous MAPA 1M, DEEA 3M and MAPA1M-DEEA3M were prepared in a volumetric flask: the required amounts of amines were weighed on a Mettler Toledo balance (model MS6002S, d = 0.01 g), and distilled water was added up to a predetermined volume and weighed. The density of the unloaded solutions was measured at 25 °C using an Anton Paar DMA 4500 M densitometer. The nominal repeatability, as given by the manufacturer, was 0.01 kg/m^3 and 0.01 °C. A detailed description of the experimental procedure is given by Pinto et al.[36] The density of the loaded solutions was measured, as reported in Perinu et al. 2018,[11] by weighing on a Mettler Toledo analytical balance (model ME204, d = 0.0001 g) 1 mL of sample (as measured by Hamilton syringes, model 1001 TLL) at room temperature. The uncertainty of this procedure was determined to be <0.6%. In Tables S1 and S2 of the Supporting Information, the densities of unloaded and loaded solutions are reported, respectively.

2.3 CO$_2$ loading

CO$_2$ loaded MAPA 1M, DEEA 3M and DEEA 3M-MAPA 1M solutions were prepared by bubbling pure CO$_2$ gas into each amine solution at room temperature. To prevent an excessive overheating of the solution, and thus water and amine loss, CO$_2$ was slowly added into the solutions. Furthermore, the concentration of the amine solutions before and after CO$_2$ bubbling

was measured and the error percentage was lower than 1.5 %, i.e. within the analytical error. The highly CO_2-loaded amine solutions were mixed with respective unloaded amine solution to obtain the predetermined CO_2 loading. To determine the CO_2 loading, the amine and CO_2 concentrations were analyzed using the titration and the precipitation methods, described in Ma'mun et al.[37]

2.4 NMR experiments

NMR is a powerful non-invasive analytical technique for chemical analyses and allows direct access to the chemical composition of CO_2 capture solvents (speciation). Chemical structures of the molecules, including unknown products and/or side-products, can be defined, and in proper performed NMR experiments the species can also be quantified.[38]

A liquid sample of each solution at different loadings was taken for NMR analysis. NMR experiments were performed at 26.85 °C on a Bruker 600 MHz Avance III HD equipped with a 5-mm cryogenic CP-TCI z-gradient probe. Qualitative 1D and 2D NMR experiments were performed to identify the species in solution, whereas quantitative ^{13}C NMR spectroscopy was applied to measure the corresponding concentration. The ^{13}C NMR spectra were acquired with the inverse gated decoupling acquisition sequence, using a recycle delay time of 120 s, a pulse width of 11.4 µs (90° pulse angle) and 256 scans. Deuterated water was used as "lock" solvent and was inside a coaxial insert, whereas Acetonitrile was chosen as internal reference standard. Further details on the method are available in previous studies. [11, 39]

2.5 pH measurements

The pH of each unloaded and loaded sample was measured using an InLab NMR pH electrode by Mettler Toledo connected to a pH meter (SevenEasy by Mettler Toledo). The calibration of the pH was performed using technical pH buffer solutions at pH 7.00, 9.21 and 11.00 provided

1   by Mettler Toledo. Each solution was inserted in an NMR tube and immersed in a thermostatic

2   water-bath (Lauda, Ecoline E100) at T = 25.0 ±0.1 °C. Before and after the measurements of

3   the CO_2-loaded amine solutions, the pH of the standard solutions was also measured as they

4   were samples, giving a pH variation of ± 0.01. In Table S3 of the Supporting Information, the

5   pH values of the solutions are reported.

6

7   **2.6 Calorimeter**

8   Differential heats of absorption of CO_2 in MAPA 1M, DEEA 3M and DEEA 3M-MAPA 1M

9   aqueous solutions were measured at 25 °C in a reaction calorimeter CPA-122 (Chemisens). To

10   validate the data, heat of absorption of CO_2 at 40 °C for MAPA 1M and DEEA 3M was

11   measured and compared to available literature data. The calorimeter is a stainless steel

12   mechanically agitated reactor with a volume of 2000 cm^3. The reactor was operated under

13   isothermal conditions and flow of heat, pressure, temperature and other parameters were

14   measured as a function of time. CO_2 was fed from two storage cylinders through a mass flow

15   controller. A detailed description of the experimental procedure is given in Kim and Svendsen[40]

16   with a small modification given in Kim et al.[41]
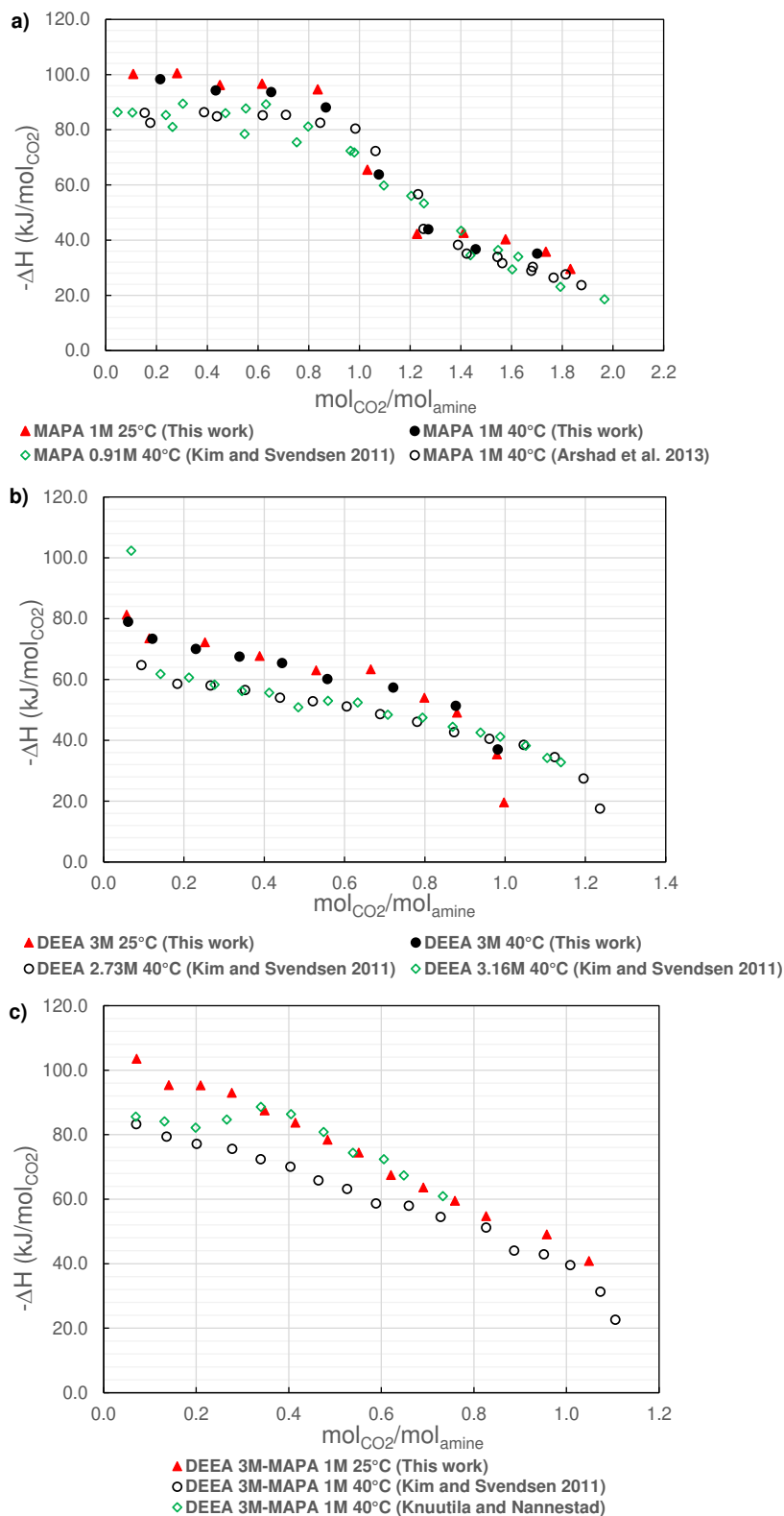
17   The experiments were initiated by evacuating the reactor to ~0.04 bar. Subsequently, around

18   1.1 - 1.2L of amine solution was fed to the reactor, and the reactor was once again evacuated

19   to degas the solution. When the system reached equilibrium, under stirring at the experimental

20   temperature, CO_2 was added to the reactor through a bottom valve. The system was left to reach

21   equilibrium before a new batch of CO_2 was fed into the solution. Equilibrium was considered

22   to be reached when there was no change in heat flow, temperature and pressure. This procedure

23   was repeated until the pressure in the reactor reached around 6 bar. At the end of the

24   experiment, a liquid sample was taken for CO_2 analysis using the precipitation and titration

25   method.[37]

1 For each injection of CO_2, equilibrium CO_2 loading (mol_{CO2}/mol_{amine}) was calculated by

2 subtracting moles of CO_2 in the gas phase from moles of CO_2 fed into the reactor, and then

3 divided by moles of amine. Moles of CO_2 fed from the CO_2 vessel and present in the gas phase

4 were calculated by Peng-Robinson equation of state, using information about pressure

5 difference and temperature in the cylinder and the reactor, respectively. The last CO_2 loading

6 deviated in average 2.4% from the CO_2 analysis. Heat of absorption was calculated by

7 integrating the heat flow curves and it was corrected for the compression-work and

8 cooling/heating effect of the incoming CO_2 gas.

9 **3. RESULTS AND DISCUSSION**

10 **3.1 Heat of absorption: comparison to literature data**

11 The differential heat of absorption of CO_2 ($-\Delta H$, kJ/mol_{CO2}) in MAPA 1M, DEEA 3M and

12 DEEA 3M-MAPA 1M solutions, measured in this work (Tables S4-S8 of the Supporting

13 Information) and in the literature, are presented in Figure 1. The results show no significant

14 difference in the heat of absorption measured at 25 and 40 °C. Overall, for MAPA and DEEA,

15 the measured heat of absorption at 40 °C as a function of CO_2 loading follows the same

16 behavior as reported in the literature.[6, 7, 40, 42] For MAPA 1M, the heat of absorption was slightly

17 higher at low CO_2 loadings, but similar after a loading of 0.6 mol_{CO2}/mol_{amine}. For DEEA, the

18 measured values were slightly higher throughout the CO_2 loading range than reported in Kim

19 and Svendsen[43] and Kim.[42] Nevertheless, the heat of absorption at 40 °C reported by Kim and

20 Svendsen[43] were also lower than those reported by Knuutila and Nannestad[6] for the blended

21 DEEA-MAPA system measured at the same temperature.

a) MAPA 1M 25°C (This work) ● MAPA 1M 40°C (This work)
◇ MAPA 0.91M 40°C (Kim and Svendsen 2011) ○ MAPA 1M 40°C (Arshad et al. 2013)

b) ▲ DEEA 3M 25°C (This work) ● DEEA 3M 40°C (This work)
○ DEEA 2.73M 40°C (Kim and Svendsen 2011) ◇ DEEA 3.16M 40°C (Kim and Svendsen 2011)

c) ▲ DEEA 3M-MAPA 1M 25°C (This work)
○ DEEA 3M-MAPA 1M 40°C (Kim and Svendsen 2011)
◇ DEEA 3M-MAPA 1M 40°C (Knuutila and Nannestad)

1

2

3 **Figure 1.** Differential heat of absorption of CO_2 in a) MAPA, b) DEEA and c) DEEA-MAPA

4 solutions.

1

3.2   Chemistry of the system and NMR analysis

In the current study, the species identified and quantified at the equilibrium in the amine systems under investigation at the different CO_2 loadings are represented in Figure 2. They are in line with the typical reaction products expected by a primary/secondary diamine and a tertiary amine in an aqueous medium in the presence of CO_2. [11, 44, 45]
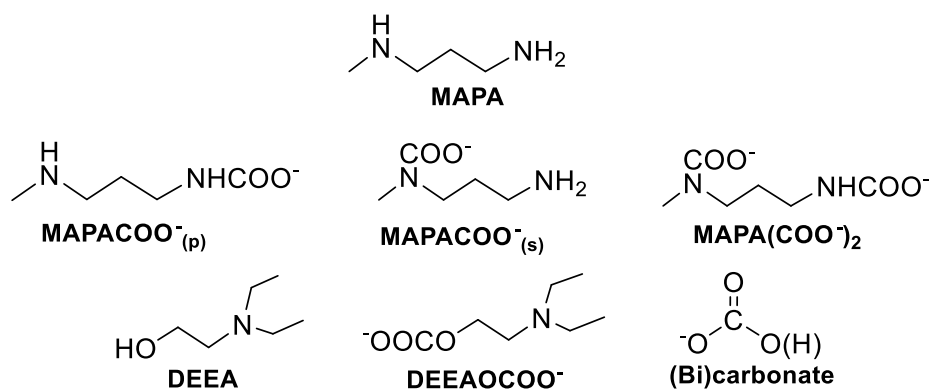

Figure 2. Chemical structure of MAPA, DEEA, their derivatives and (bi)carbonate in the aqueous solutions in the presence of CO_2. Each species is in equilibrium with the corresponding protonated form.

MAPA/MAPAH$^+$/MAPA(H$^+$)$_2$ (simply reported as MAPA/MAPA(H$^+$)$_2$ along the manuscript and in the graphs), primary MAPA carbamate (MAPACOO$^-_{(p)}$/MAPAH$^+$COO$^-_{(p)}$), secondary MAPA carbamate (MAPACOO$^-_{(s)}$/MAPAH$^+$COO$^-_{(s)}$) and MAPA(COO$^-$)$_2$ are the species identified in the amine systems containing MAPA; DEEA/DEEAH$^+$ and tertiary amino carbonate (DEEAOCOO$^-$/DEEAH$^+$OCOO$^-$) are identified in single and blended DEEA; and (bi)carbonate species (HCO$_3^-$/CO$_3^{2-}$) is found in all the systems. Details on the corresponding concentrations (mol/L) can be found in the Supporting Information (Tables S9-S11).

In the ^{13}C NMR spectra, the signals corresponding to carbons of the protonated and neutral form of each species (free/protonated amines and/or HCO$_3^-$/CO$_3^{2-}$) appear with a common signal because, at the selected temperature, the proton exchange is faster than the NMR time

scale. The chemical shifts (expressed in ppm) depend on their ratio and, in the case of HCO_3^-

and CO_3^{2-}, they can span from about 161.1 ppm for 100% HCO_3^- to about 168.7 ppm for 100%

CO_3^{2-}.[39] In this study, an estimation of the HCO_3^- and CO_3^{2-} content was performed by applying

the method developed by Perinu et al. [39]

To verify the reliability of the NMR data, the CO_2 loadings as measured by NMR and by

titration-precipitation method were compared (Figure 3). The measurements obtained by both

methods were fitting quite well, except for one point in a loaded solution of MAPA 1M.

Specifically, at the 7th CO_2 loading (0.94 mol_{CO2}/mol_{amine}), as measured by using the titration-

precipitation method, and at 0.81 mol_{CO2}/mol_{amine}, as measured by NMR analysis, there is a

mismatch. The reason may be related to the fact that the peak corresponding to the HCO_3^-

/CO_3^{2-} species was not identified in the NMR spectra, although this species might be present.

It may be possible that the peak corresponding to the (bi)carbonate species is overlapped with

the carbon-peak of the carboxylate ion of a MAPA carbamate species.
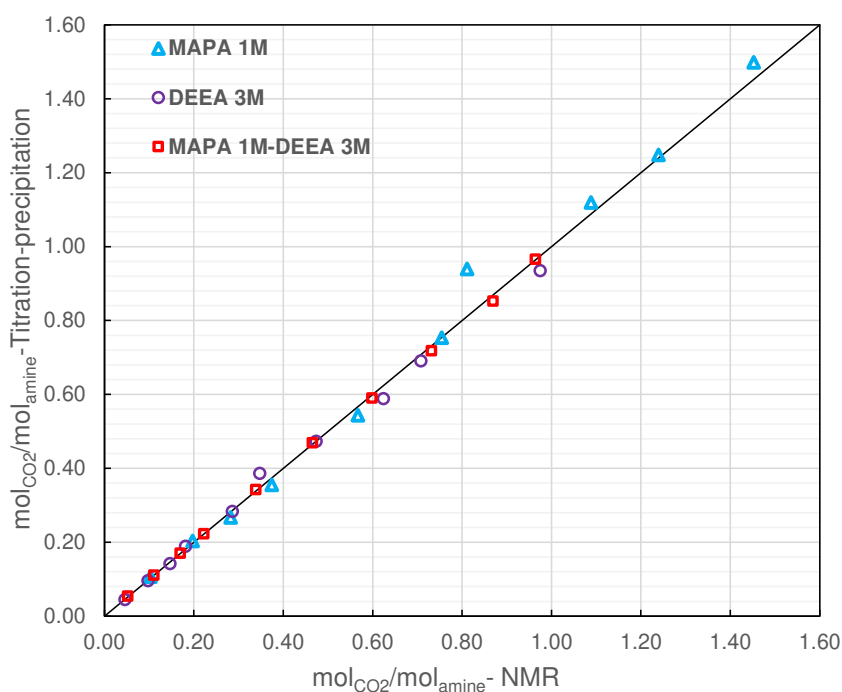
Figure 3. Comparison of mol_{CO2}/mol_{amine} as measured by NMR and by titration-precipitation
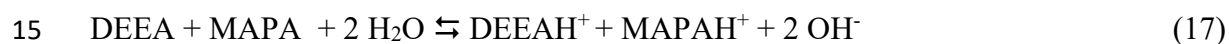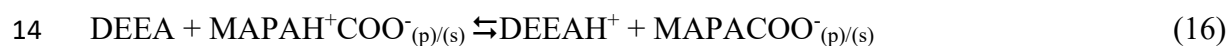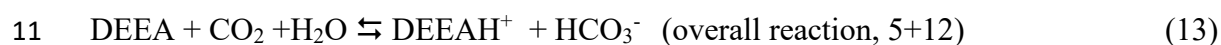
analyses.

The identification and quantification of the species and the interrelation with pH and heat of absorption data allowed defining a list of reactions occurring in the solvents under investigation. For sake of clarity, all the reactions discussed in each section are here listed, but they are not in the order they may occur in the different systems:
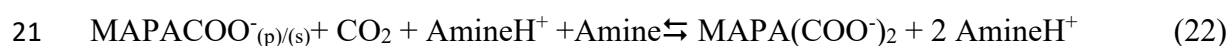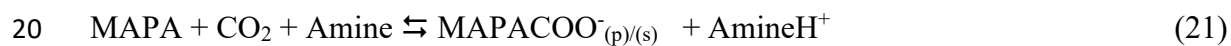
CO$_2$-H$_2$O reactions

Reactions (5), (6), (7) (see section 1.1)

$H_2O \leftrightarrows H^+ + OH^-$ (10)

$CO_3^{2-} + CO_2 + H_2O \leftrightarrows 2\ HCO_3^-$ (11)

DEEA reactions

$DEEA + H_2O \leftrightarrows DEEAH^+ + OH^-$ (12)

$DEEA + CO_2 + H_2O \leftrightarrows DEEAH^+ + HCO_3^-$ (overall reaction, 5+12) (13)

$DEEA + HCO_3^- \leftrightarrows DEEAOCOO^- + H_2O$ (14)

$DEEA + MAPA(H^+)_2 \leftrightarrows DEEAH^+ + MAPAH^+$ (15)

$DEEA + MAPAH^+COO^-_{(p)/(s)} \leftrightarrows DEEAH^+ + MAPACOO^-_{(p)/(s)}$ (16)

$DEEA + MAPA + 2\ H_2O \leftrightarrows DEEAH^+ + MAPAH^+ + 2\ OH^-$ (17)

MAPA reactions

$MAPA + H_2O \leftrightarrows MAPAH^+_{(p/s)} + OH^-$ (18)

$MAPAH^+_{(p/s)} + H_2O \leftrightarrows MAPA(H^+)_2 + OH^-$ (19)

$MAPA + CO_2 \leftrightarrows MAPAH^+COO^-_{(p)/(s)}$ (20)

$MAPA + CO_2 + Amine \leftrightarrows MAPACOO^-_{(p)/(s)} + AmineH^+$ (21)

$MAPACOO^-_{(p)/(s)} + CO_2 + AmineH^+ + Amine \leftrightarrows MAPA(COO^-)_2 + 2\ AmineH^+$ (22)

$MAPA(COO^-)_2 + H_2O + H^+ \leftrightarrows MAPAH^+COO^-_{(p)/(s)} + HCO_3^-$ (23)

$MAPACOO^-_{(p)/(s)} + H_2O + H^+ \leftrightarrows MAPAH^+_{(p/s)} + HCO_3^-$ (24)

$MAPAH^+COO^-_{(p)/(s)} + H_2O + H^+ \leftrightarrows MAPA(H^+)_2 + HCO_3^-$ (25)

1 Reaction 10 is neither discussed nor mentioned during the discussion of the results, as it is

2 considered to be a default reaction. In the reactions 21 and 22, the "Amine" acting as counter-

3 ion (stronger Brønsted base) may change as a function of the solvents investigated. In reaction

4 20, the nitrogen of $MAPAH^+COO^-_{(p)/(s)}$ not bound to CO_2 is protonated and acts as counterion

5 of the $-COO^-$ group.

6

7 **3.3   Analysis of NMR speciation, pH and ΔH data**

8 **3.3.1 DEEA 3M-CO_2-H_2O system**

9 The concentration (mol/L) of all the species formed in aqueous DEEA 3M, in the presence of

10 different addition of CO_2, are plotted together with pH data (Figure 4).
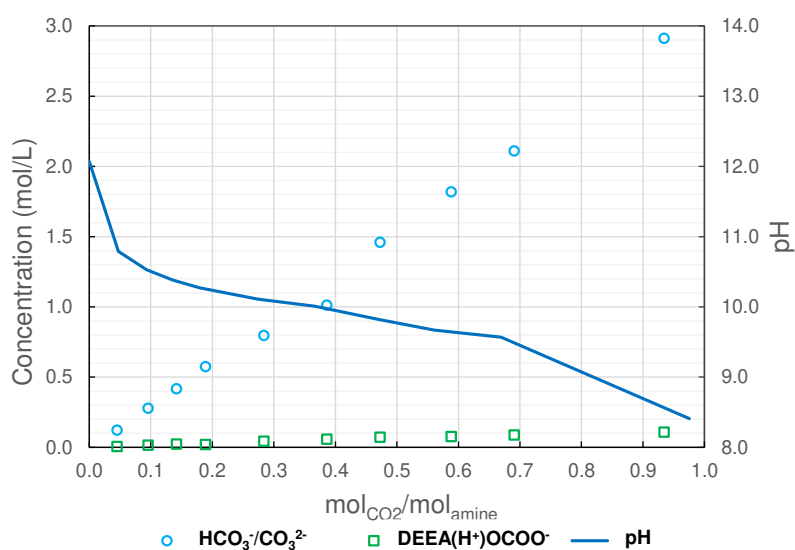

11

12 **Figure 4.** NMR speciation and pH data in aqueous DEEA 3 M at increasing CO_2 loading (25

13 °C).

14

15   (Bi)carbonate (HCO_3^-/CO_3^{2-}) and $DEEAOCOO^-$ are the two CO_2-containing species present

16 at the equilibrium at the different loadings.

1   DEEAOCOO[-] is found in negligible amount and it appears to have the tendency of increasing

2   at increasing addition of CO_2, as for MDEAOCOO[-] in the study on CO_2 loaded MDEA in

3   water by Behrens et al.[21]

4   As expected, (bi)carbonate species are the main product of the CO_2 absorption and the total

5   concentration of HCO_3^- and CO_3^{2-} constantly increases since the beginning of the loading. In

6   this system, from 0.04 $molCO_2/mol_{amine}$ to about 0.59-0.69 $molCO_2/mol_{amine}$, the chemical

7   shifts were ranging from 165.7 ppm to 162.8-162.3 ppm, respectively, and so were consistent

8   with the presence of both HCO_3^- and CO_3^{2-}, with the HCO_3^- content increasing at increasing

9   loading. At the maximum loading, the chemical shift value (161.3 ppm) is instead consistent

10   with the predominant presence of HCO_3^- (the chemical shifts corresponding to HCO_3^-/CO_3^{2-}

11   signal are available in the Table S12 of the Supporting Information). In terms of concentrations,

12   the Figure 5 shows that, at increasing loading, the amount of HCO_3^- constantly increases,

13   whereas the amount of CO_3^{2-}, mainly in concentrations lower than HCO_3^-, increases until a

14   loading of around 0.47 $molCO_2/mol_{amine}$ before it starts being consumed.
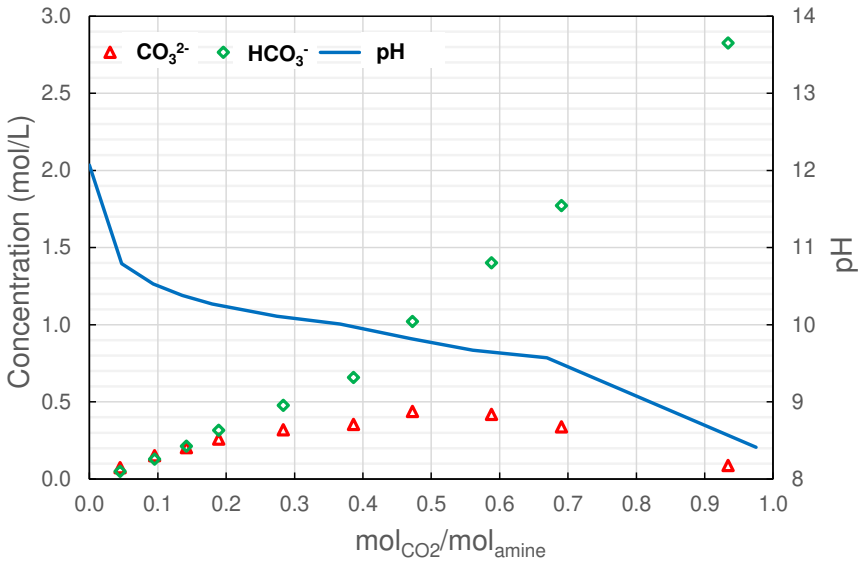
15

16   **Figure 5.** Estimation of the HCO_3^- and CO_3^{2-} content in aqueous DEEA 3M.

17   The pH values span from pH 12.07 at 0.00 mol_{CO2}/mol_{amine} to pH 8.41 at maximum loading,

18   and it shows a constant decrease, with some changes in the slope of the curve. We observe a

1

1   drop of $\Delta pH=1.28$ in the range between the 0.0 $mol CO_2/mol_{amine}$ and 0.05 $mol CO_2/mol_{amine}$,

2   due to the first addition of the acid CO_2, and another of $\Delta pH=1.16$ in the last loadings-region,

3   between 0.67 and 0.98 mol_{CO2}/mol_{amine}, where the basicity of the solution greatly decreases as

4   the majority of the amines are protonated. DEEA/DEEAH$^+$ is a buffer system made of a weak

5   acid (DEEAH$^+$) and its conjugate base (DEEA). When the pH of the solution is lower than the

6   pK_a value of an amine, the larger part of the amine is protonated and cannot act as a catalyst of

7   CO_2 hydration.[30] In this study, at about 0.47 mol_{CO2}/mol_{amine}, the pH of the solution is 9.8 and,

8   from here onward, it becomes lower than the pK_a value of DEEA (9.84). Hence, the amine

9   capacity, in terms of amount of conjugate base (DEEA), is reduced, i.e. the basicity of the

10   amine solution is weaker, and since the concentration of CO_3^{2-} starts to be diminished, it can

11   be concluded that CO_3^{2-} also reacts as a conjugate base,[24, 46] as reported in reaction 11 (similarly

12   to the generic reaction 4 or the DEEA-specific reaction 13).

13   Concerning the heat of absorption (Figure 6), as general tendency, at increasing loading a

14   steady and slight decrease is observed.
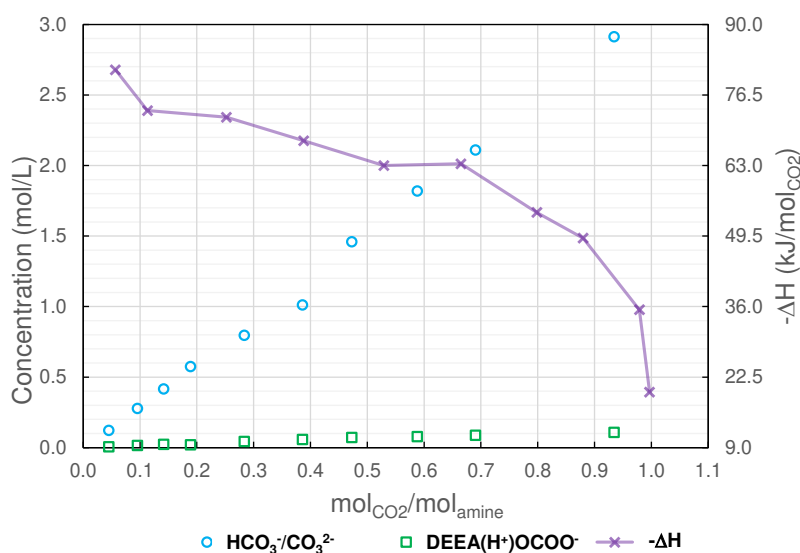
15

16   **Figure 6.** NMR speciation and heat of absorption data in aqueous DEEA 3 M at increasing

17   CO_2 loading (25 °C).

However, similarly to the pH curve, a rapid drop off occurs in the last-loading region, from about 0.67 mol_{CO2}/mol_{amine} onward, which can hence be defined as the saturation loading region.[47] Due to the reduction of the amine capability as conjugate base, alternative pathways for the bicarbonate formation and/or CO_2 capturing (like e.g. reaction 11) may go along and show to release less heat than the reactions occurring before the saturation region. Accordingly, the $DEEAOCOO^-$ tendency of increasing at increasing loading may also be attributable to the saturation of the amine nitrogen capabilities. In this study, its formation is generically represented by the reaction 14 since, with the data available, it was not possible to investigate the reaction mechanisms of this species.

In summary, alongside the addition of CO_2, the reactions 13 and 14 are mainly occurring. Reaction 13 represents the catalysis of the reaction 7 and it sums up the reactions 5 and 12. Moreover, until about 0.5 mol_{CO2}/mol_{amine}, which corresponds to pH$\geq$9.8, the reaction 6, leading to CO_3^{2-} species, also takes place; from here to the maximum loading (pH<9.8), the CO_3^{2-} is instead consumed as represented in the reaction 11.

3.3.2 MAPA 1M-CO₂-H₂O system

In Figure 7, the speciation of the aqueous diamine MAPA 1M at increasing CO_2 addition is reported together with the pH measurements.
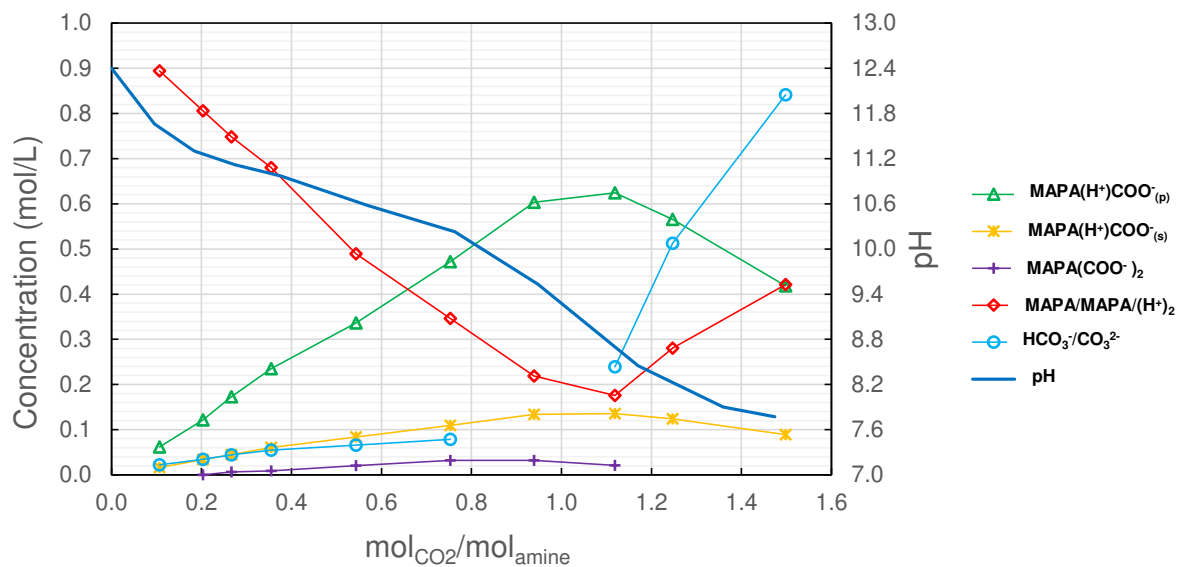

Figure 7. NMR speciation and pH data in aqueous MAPA 1M at increasing CO_2 loading (25 °C).

As soon as the solution is loaded with CO_2, MAPA/MAPA$(H^+)_2$ starts decreasing to form primary and secondary MAPA carbamate (MAPA$(H^+)COO^-_{(p)}$ and MAPA$(H^+)COO^-_{(s)}$, respectively), as described in the reactions 20 and 21. The constant increase of MAPA$(H^+)COO^-_{(p)}$ and MAPA$(H^+)COO^-_{(s)}$ at increasing loading is evident until around 0.94 mol_{CO2}/mol_{amine}. Around this point, a sort of stabilization in the increase of these two species is observed, and from around 1.12 mol_{CO2}/mol_{amine} onward, their concentration decreases, i.e. hydrolysis reactions 24-25 occur.

MAPA$(COO^-)_2$ is formed (reaction 22) in amounts in the order of the second decimal number and much lower than MAPA$(H^+)COO^-_{(p)/(s)}$. At beginning of CO_2 loading, the corresponding peaks in the ^{13}C NMR spectra are not observed. From around 0.20 mol_{CO2}/mol_{amine} to 0.36 mol_{CO2}/mol_{amine} only traces (lower than 0.01 mol/L) are formed, and its amount increases until

around 0.75-0.94 mol_{CO2}/mol_{amine}. Around this region, the concentration is quite stable, and from 0.94 mol_{CO2}/mol_{amine} onward, a decrease (hydrolysis reaction, as shown in reaction 23) is observed.

In a previous NMR study on 0.5 M and 1M MAPA, the species $MAPA(COO^-)_2$ was also found in negligible amount.[11] The reason is that the nitrogen not bound to CO_2 in $MAPACOO^-_{(p)/(s)}$ may not be available for reaction with CO_2 because, as given in reaction 20, it could be protonated and act thus as counterion to the negative charged groups. The concentration of $MAPA/MAPA(H^+)_2$ constantly decreases until around 1.12 mol_{CO2}/mol_{amine} and, from here onward, it starts increasing due to the hydrolysis of $MAPA(H^+)COO^-_{(p)}$ and $MAPA(H^+)COO^-_{(s)}$. Not all the MAPA in solution reacts with CO_2 as it also goes through the reaction of protonation (Reaction 18 and 19) and, in the protonated form, it can act as counter ion, like e.g. in reaction 21 and 22 the "Amine" may be MAPA.

(Bi)carbonate is formed throughout the CO_2 loading range. It is mainly in concentration higher than $MAPA(COO^-)_2$ and lower than $MAPACOO^-_{(p)}$ but, around the region of the maximum mol_{CO2}/mol_{amine}, it reaches concentrations higher than all the species in solution. Specifically, its presence is more evident from the region of hydrolysis onward (at loading 0.94 the HCO_3^- /CO_3^{2-} signal was not detected because it was probably overlapped with the carbamate signals).

Concerning the pH, it decreases at increasing CO_2 loading. As soon as CO_2 is added into the solution, a ΔpH drop of 0.74 is observed and, during the CO_2 addition, the pH values span from 11.66 at about 0.1 mol_{CO2}/mol_{amine} to 7.77 at about 1.5 mol_{CO2}/mol_{amine}. A change in the slope of the curve is observed at about 0.76-1.17 mol_{CO2}/mol_{amine} and, specifically, a unit pH drop occurs between 0.95 and 1.17 mol_{CO2}/mol_{amine}, which is the region where the MAPA carbamates hydrolyses start.

The hydrolyses of MAPA carbamate species occurred at about pH 9.5 and the reactions 23-25 show how they may be driven by the acidity of the solution. The reaction of the nitrogen atom

of the amine carbamates with a proton makes the compound unstable, leading to the formation of protonated MAPA species and HCO_3^-. Alike, in a study by Lv et al.[34] it was reported that the hydrolysis of MEA carbamate was occurring at about pH 9. Similarly, Zhang et al.[10] in the study of CO_2 loaded aqueous solution of MAPA 2M at 40 °C, showed that the reactions of carbamate hydrolysis started at about pH 9.5. The speciation trends in MAPA 2M are comparable to those observed in our study, but due to the different reaction conditions and concentrations, some differences are observed. In the present study, a lower end pH value at the same loading (1.5 mol_{CO2}/mol_{amine}) was reached since the work is dealing with MAPA 1M aqueous solution as compared to MAPA 2M. Hence, with respect to $MAPACOO^-_{(p)}$, more (bi)carbonate than reported by Zhang et al. is observed. Moreover, in our study, at the pH value of the carbamate hydrolysis, not all the MAPA in solution has reacted with CO_2, as it was instead for MAPA 2M in Zhang et al.[10]

In Figure 8, the concentration of the species in aqueous MAPA 1M at increasing CO_2 loading are reported together with the heat of absorption.
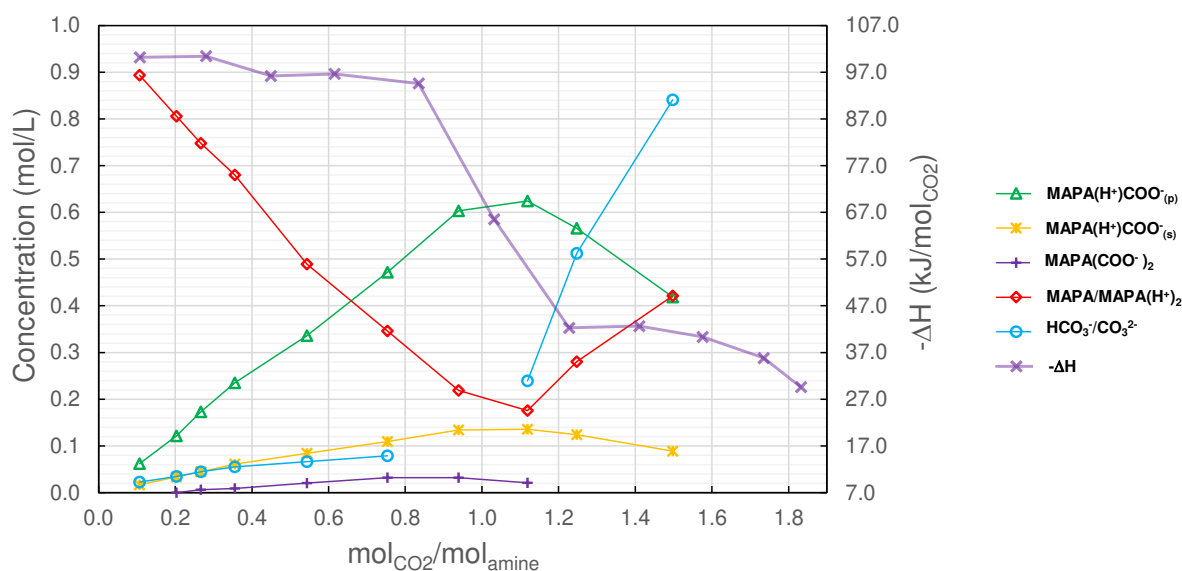
Figure 8. NMR speciation and heat of absorption data in aqueous MAPA 1M at increasing CO_2 loading (25 °C).

The heat of absorption is quite constant and stays approximately the same until 0.84 mol_{CO2}/mol_{amine}, where a sudden dropping off is observed (0.84-1.23 mol_{CO2}/mol_{amine}). Carbamate is known to be an exothermic reaction releasing high heat of reaction, and the heat released decreases as soon as the hydrolysis occurs and/or the carbamate is not formed anymore.

Hence, in the range of the CO_2 loading (from the beginning to the maximum loading), two main regions can be identified:

1) In the first region, going from about 0.11 to about 0.94 mol_{CO2}/mol_{amine}, the following reactions are mainly occurring:

   - Protonation of MAPA (reaction 18-19);

   - Formation of primary and secondary MAPA carbamate (reaction 20-21), and in negligible amount, formation of $MAPA(COO^-)_2$ (reaction 22).

   - Formation of (bi)carbonate in small amount through the reactions 5-7. Additionally, MAPA may act by providing basicity (reaction 18-19), leading to a kind of CO_2 hydration catalysis (reaction 4) (as DEEA singly in reaction 13). However, in MAPA solution, the carbamate formation is favored.

2) In the second region, from about 0.94 mol_{CO2}/mol_{amine} onward, the hydrolysis reactions mainly take place:

   - Around 0.94-1.25 mol_{CO2}/mol_{amine}, the hydrolysis of $MAPA(COO^-)_2$ (reaction 23) occurs;

   - Around 1.12-1.5 mol_{CO2}/mol_{amine}, the hydrolyses of primary and secondary MAPA carbamate (reactions 24 and 25) are predominant;

   - (Bi)carbonate found in solution is mainly coming from the reactions of amine carbamate hydrolysis (23-25), but the reactions 5, 7 and 11 may also take place (reaction 5 is however negligible at pH lower than 8^{25}). Reaction 11 is supported by

the chemical shift value of the peaks corresponding to the HCO_3^-/CO_3^{2-} species in the ^{13}C NMR spectra. The ppm values are consistent with the presence of both CO_3^{2-} and HCO_3^- until about 1.12 mol_{CO2}/mol_{amine}. From here onward, the ppm values are in line with the only presence of HCO_3^- (the chemical shifts and the estimated concentrations are available in Table S11 and in Figure S1 of the Supporting Information, respectively).

3.3.3 MAPA 1M-DEEA 3M-CO₂-H₂O system

In Figure 9, the amount of each species in MAPA 1M-DEEA 3M-CO_2-H_2O is reported for each

CO_2 loading and interrelated with pH data.
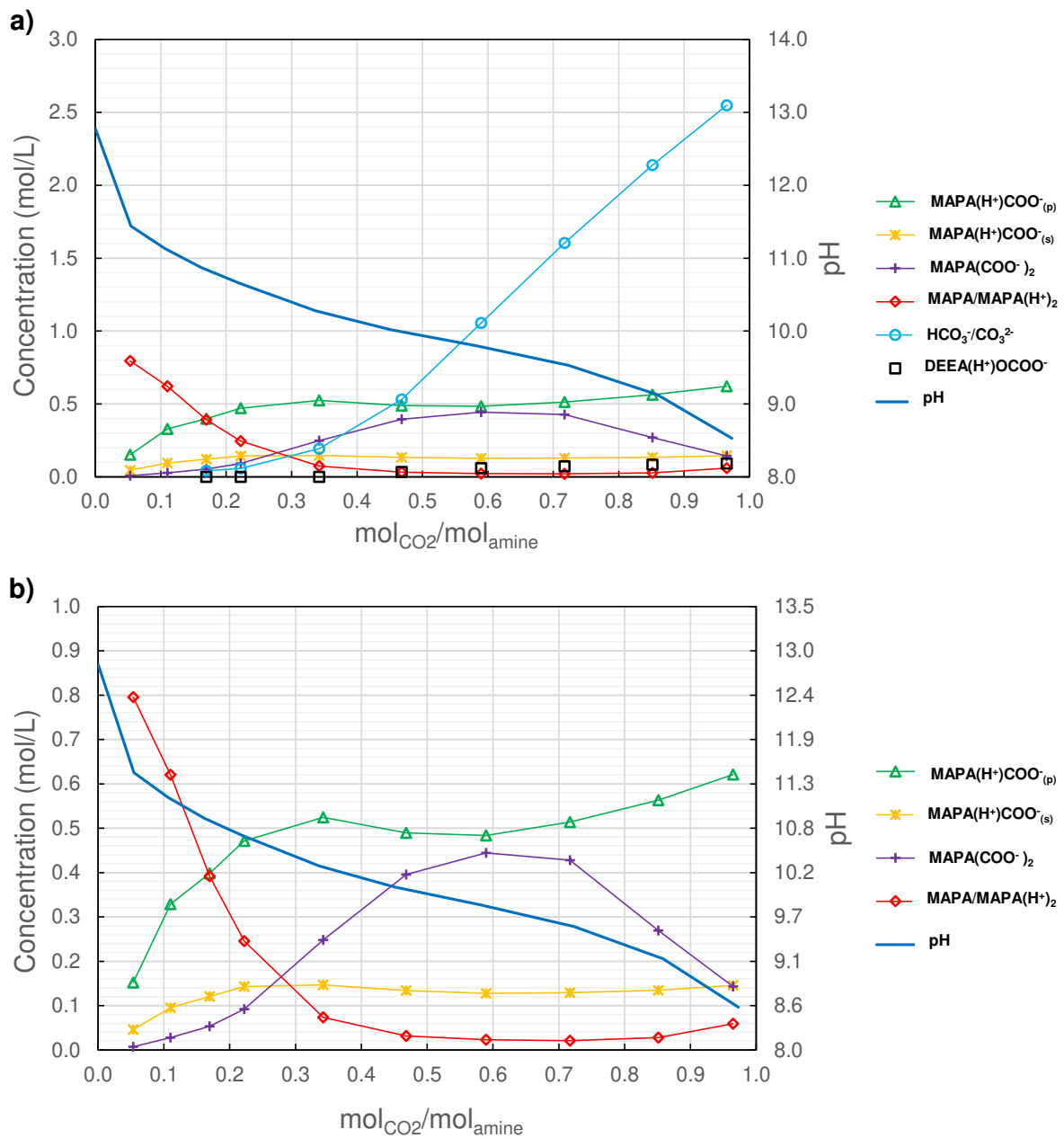
Figure 9. Concentration of a) all the species and b) MAPA derivative species only, and pH

data in aqueous MAPA 1M-DEEA 3M at increasing CO_2 loading (25 °C).

The same species observed in MAPA 1M and DEEA 3M are found, but at different concentrations and ratios.

DEEAOCOO$^-$ (given by reaction 14) has a trend like that observed in DEEA 3M, but it is not detected since the early loadings.

MAPACOO$^-_{(p)}$ and MAPACOO$^-_{(s)}$, given by reactions 20-21, increase until around loading 0.34 mol$_{CO2}$/mol$_{amine}$. In the region around 0.34-0.59 mol$_{CO2}$/mol$_{amine}$ a slight decrease and/or stabilization of their concentrations is observed, whereas from 0.59 mol$_{CO2}$/mol$_{amine}$ onward an increase is again observed. From about 0.22 mol$_{CO2}$/mol$_{amine}$ until around 0.59 mol$_{CO2}$/mol$_{amine}$, the concentration of MAPA(COO$^-$)$_2$ (formed as in reaction 22) deeply increases to the detriment of MAPACOO$^-_{(p)/(s)}$. From 0.59 mol$_{CO2}$/mol$_{amine}$ until maximum loading, it goes through the hydrolysis process (reaction 23) and, therefore, decreases in favor of formation of further MAPACOO$^-_{(p)/(s)}$.

MAPA is almost totally consumed and the curve shows a steep decrease until loading 0.34 mol$_{CO2}$/mol$_{amine}$, (region where MAPA(H$^+$)COO$^-_{(p)/(s)}$ do not show any more a steep increase). From here to 0.72 mol$_{CO2}$/mol$_{amine}$, the decrease becomes slightly less evident, and it starts slightly increasing from 0.72 mol$_{CO2}$/mol$_{amine}$ to the maximum loading. The hydrolysis of MAPACOO$^-_{(p)/(s)}$ may go along that of MAPA(COO$^-$)$_2$, but its evidence is only given around the last-loadings region where a slight increase of MAPA is observed.

Concerning the pH trend, it has the tendency of decreasing at increasing addition of CO$_2$. Specifically, throughout the CO$_2$ loading range, the pH spans from 11.44 at 0.05 mol$_{CO2}$/mol$_{amine}$ to 8.53 at maximum loading. A clear drop is observed between 0.00 and 0.05 mol$_{CO2}$/mol$_{amine}$ (ΔpH=1.34), and the curve gets slightly steeper close to the maximum loading. However, similarly to MAPA 1M, the amine carbamate hydrolysis starts at pH less than 10, i.e. about pH 9.8.

1   In Figure 10, the heat of CO_2 absorption in blend has been interrelated with the concentrations

2   of the MAPA-derivative species.
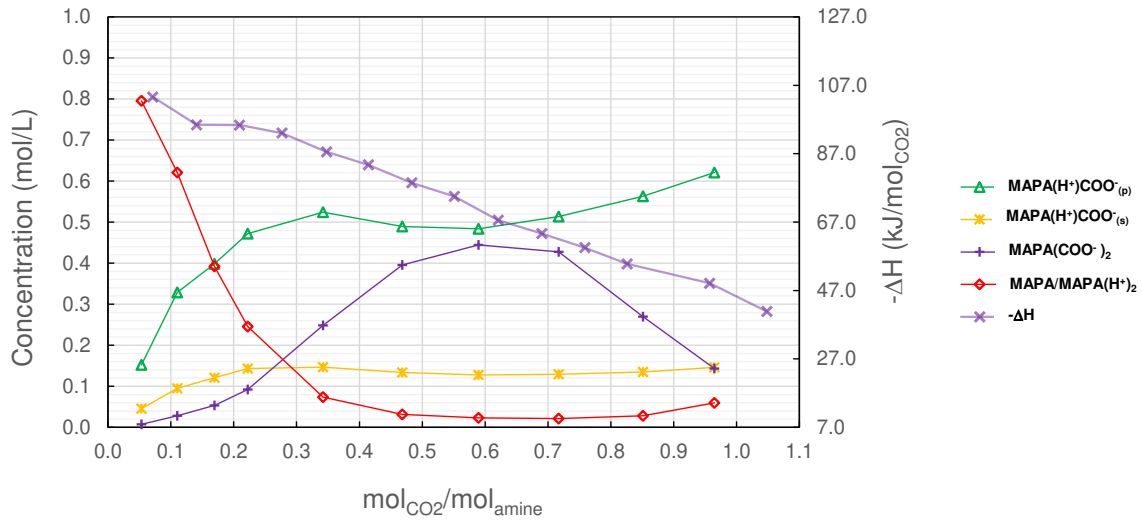
3

4   **Figure 10.** Concentration of MAPA-derivative species at different CO_2 loadings (25 °C) and

5   heat of absorption trends in aqueous MAPA1M-DEEA3M.

6

7   Throughout the CO_2 loading range, the heat continues to decrease steadily without any evident

8   drop. Rather, the heat of absorption appears not to be influenced by the carbamate hydrolysis

9   as it was instead observed in MAPA 1M.

10   The heat released by the DEEA-activity may somehow compensate the heat released by the

11   carbamate formation, and it may lead to an absence of a rapid drop off in the region of

12   carbamate hydrolysis. For clarifying the behavior, in the Figure 11, the (bi)carbonate

13   concentrations and the heat of absorption at the different CO_2 loadings in the three systems are

14   compared.
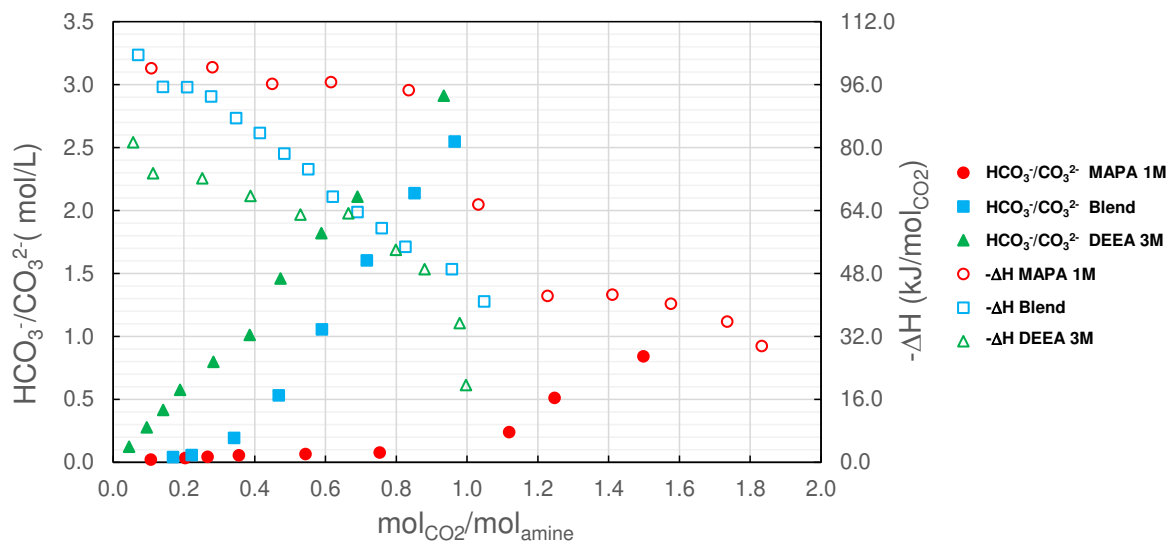
Figure 11. Comparison of (bi)carbonate and heat of absorption in MAPA 1M, DEEA 3M and their blend.

In the blend, until about 0.34 mol_{CO2}/mol_{amine}, the concentrations of (bi)carbonate is more like MAPA 1M than DEEA 3M, indicating that the activity of DEEA as Brønsted base has not yet an influence on the bicarbonate formation (as it is in DEEA 3M). Such activity is more evident from 0.34 mol_{CO2}/mol_{amine} onward, where the (bi)carbonate species has the same trend as DEEA 3M, but still lower concentrations. Similarly, the heats of absorption in MAPA 1M and MAPA 1M-DEEA 3M were comparable and almost constant until about 0.3 mol_{CO2}/mol_{amine}. From here, in MAPA 1M-DEEA3M it constantly decreased, while in MAPA 1M it stayed approximately the same until a loading of about 0.84 mol_{CO2}/mol_{amine}, the region where the amine carbamate hydrolyses take place.

The speciation data shown in Figures 9-11 represents the thermodynamic composition of the solution at the specific CO_2 loading reported. In the case of the blend, until around 0.34 mol_{CO2}/mol_{amine}, we observe (Figure 9) that primary MAPA carbamate is the main product, followed by secondary MAPA carbamate and finally MAPA(COO$^-$)$_2$. From about 0.34 mol_{CO2}/mol_{amine}, along with formation of amine carbamates, further addition of CO_2 contributes

1 to HCO_3^-/CO_3^{2-} formation, which is probably due to activity of DEEA as a Brønsted base.

2 Moreover, from 0.59 mol_{CO2}/mol_{amine} onwards, MAPA carbamate hydrolysis reactions also

3 contribute to bicarbonate formation. A similar situation is observed for 1M MAPA at

4 approximately 0.8 mol_{CO2}/mol_{amine} (Figure 7 and 8). For MAPA 1 M this point corresponds to

5 a significant drop in ΔH and pH indicating a change in formation of the predominant reaction

6 product, i.e. towards bicarbonate. In the blend, the presence of 3M DEEA seems to blanket this

7 clear change, and as soon as the trend for (bi)carbonate formation goes as in DEEA 3M, the

8 released heat steadily decreases. However, due to the formation of the MAPA carbamate

9 species, it is still higher than in the single DEEA 3M, as well as the amount of (bi)carbonate is

10 lower.

11 Moreover, to have a visual picture of DEEA's activity and influence on MAPA, the MAPA

12 derivative species both in blend and in MAPA 1M are plotted as a function of mol_{CO2}/mol_{MAPA}

13 (Figure 12).
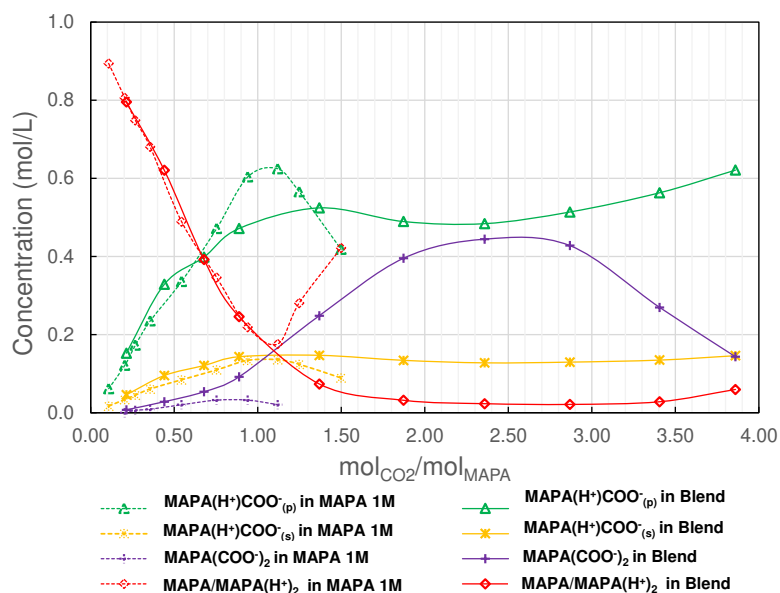
14

15 **Figure 12.** Comparison of MAPA derivatives species in single and blended aqueous MAPA

16 1M as a function of mol_{CO2}/mol_{MAPA}

17

It is possible to observe that the speciation curves for both single and blended MAPA are similar until around 0.7 mol_{CO2}/mol_{MAPA}. Around this loading, in MAPA 1M the species MAPA(H$^+$)COO$^-_{(p)}$ continues increasing, while in the blend its concentration goes towards a stabilization in favor of MAPA(COO$^-$)$_2$ formation. Around 1.1 mol_{CO2}/mol_{MAPA}, in MAPA1M the carbamate hydrolysis of MAPA(H$^+$)COO$^-_{(p)/(s)}$ starts, while MAPA species in the blend continue to react with CO_2 (e.g. MAPA(COO$^-$)$_2$ starts swiftly increasing).

At increasing CO_2 loading, the amino-sites for absorbing CO_2 are saturated (not available), the pH decreases, and the carbamate hydrolysis starts. In the presence of DEEA, MAPA is almost totally consumed, meaning that the amino functional groups are more available for the reactions of carbamate formation, and MAPA is then less protonated. The same is true for the amino functional groups not bound to CO_2 in MAPACOO$^-_{(p)/(s)}$.

Then, in the present study, the role played by DEEA in the presence of MAPA and CO_2 confirms the findings reported by Perinu et al.[11] for MAPA in blend with several tertiary amines. Specifically, DEEA (pK$_a$=9.84), having the pK$_a$ value larger than pK$_{a2}$ of MAPA (pK$_{a1}$= 10.6 and pK$_{a2}$=8.6), may withdraw protons from protonated MAPA species (reactions 15-16) and/or lead the protonation process (reaction 12 and 17), and in the protonated form it acts as counter ion of the carbamate species (the term "Amine" in reactions 21-22). Jang et al. 2018 also concluded that DEEA, and generally the tertiary amines, can induce the reaction from protonated MEA to active molecule MEA.[48]

To summarize, in the blend with MAPA, the Brønsted base DEEA plays two main roles in the presence of CO_2. It acts both by increasing the availability of MAPA's nitrogens to form carbamates (e.g., MAPA(COO$^-$)$_2$ is formed in significant amount as compared to single MAPA, where its concentration is negligible), and by catalyzing the hydration of CO_2 for (bi)carbonate formation (as it is in the absence of MAPA).

Based on the above results and discussion, during the addition of CO_2 in aqueous MAPA 1M-DEEA 3M, three main regions can be identified:

1) In the first region, spanning from 0.05 to 0.34 mol_{CO2}/mol_{amine}, the following reactions take place:

- Amines protonation, i.e. MAPA protonation reactions (18-19), together with the exchange-proton reactions with DEEA (reactions 15-17).

- Reactions 20-22 which lead to formation of MAPA carbamates.

- (Bi)carbonate is formed in small amount, and the reactions 5 and 6 may mainly occur (pH is higher than 10 and DEEA is not yet involved in the CO_2 hydration catalysis).

2) The second region can be identified around 0.34-0.59 mol_{CO2}/mol_{amine}:

- Formation of $MAPA(COO^-)_2$ (reaction 22)

- The DEEA has similar activity as in DEEA 3M.

3) In the third region (0.59-0.96 mol_{CO2}/mol_{amine}), carbamate hydrolysis reactions are mainly occurring:

- $MAPA(COO^-)_2$ hydrolysis is predominant (Reaction 23),

- Hydrolysis of $MAPA(H^+)COO^-_{(p)/(s)}$ (reactions 24-25) may be considered a minor one

- Along with the reactions as in DEEA 3 M singly, (bi)carbonate found in solution is coming from the carbamate hydrolysis (reactions 23-25). The reaction 11 may also occur and it is supported by the chemical shift values of HCO_3^-/CO_3^{2-} and corresponding concentrations (see the chemical shift values in Table S11 and the estimated concentrations in Figure S2 of the Supporting Information).

4. CONCLUSIONS

In this study, aqueous MAPA 1M, DEEA 3M and their blend were investigated in the presence of CO_2. Based on speciation, heat of absorption and pH data analyses, the main reactions occurring at various CO_2 addition were identified and discussed.

At increasing CO_2 loading, the basicity of the solution decreases, as well as the capability of each amine to absorb CO_2. In the aqueous MAPA systems, this leads to the hydrolysis of the carbamate species, which also corresponds to a drop in the released heat. The reactions of carbamate hydrolysis in both single and blended MAPA occur at similar pH values (i.e. about pH 9.8-9.5), but in the blended MAPA, due to the activity of DEEA, the drop in both pH and heat of absorption is not so noticeable as in MAPA singly. The Brønsted basicity of DEEA indeed acts both by catalyzing the CO_2 hydration reaction and by allowing the diamine to be more available for the direct reaction to CO_2, i.e. carbamate formation.

In the investigated amine systems, a saturation region can be identified in the region close to the maximum loading, and it is observed when the amine capability, in terms of conjugate Brønsted base and/or Lewis base, is reduced and/or saturated.

With the present study, crucial insights for MAPA and DEEA solvents, singly and in blend, are given and can be considered valuable for the selection of new amine solvents with improved properties.

ASSOCIATED CONTENT

Supporting Information. The following file is available free of charge. Density, pH, heat of absorption, NMR speciation, chemical shifts and estimated concentration of bicarbonate and carbonate species (PDF).

AUTHOR INFORMATION

Corresponding Author

*Email: klaus.j.jens@usn.no

Notes

The authors declare no competing financial interest.

REFERENCES

(1) IPCC, *Climate Change 2014: Synthesis Report.* Contribution of Working Groups I, II and III to the Fifth Assessment Report of the Intergovernmental Panel on Climate Change [Core Writing Team, R.K. Pachauri and L.A. Meyer (eds.)]. IPCC, Geneva, Switzerland, 2014.

(2) Rochelle, G. T. Amine Scrubbing for CO_2 Capture. *Science* **2009**, *325* (5948), 1652-1654.

(3) Reynolds, A. J. Verheyen, T. V.; Adeloju, S. B.; Meuleman, E.; Feron, P., Towards Commercial Scale Postcombustion Capture of CO_2 with Monoethanolamine Solvent: Key Considerations for Solvent Management and Environmental Impacts. *Environ. Sci. Technol.* **2012**, *46* (7), 3643-3654.

(4) Puxty, G.; Maeder, M. 2 - The fundamentals of post-combustion capture A2 - Feron, Paul H.M. In *Absorption-Based Post-combustion Capture of Carbon Dioxide*, Woodhead Publishing, 2016.

(5) Hwang, S. J.; Lee, M.; Kim, H.; Lee, K. S. Cyclic CO_2 absorption capacity of aqueous single and blended amine solvents. *J. Ind. Eng. Chem.* **2018**, 65, 95-103.

(6) Knuutila, H. K.; Nannestad, Å. Effect of the concentration of MAPA on the heat of absorption of CO_2 and on the cyclic capacity in DEEA-MAPA blends. *Int. J. Greenhouse Gas Control* **2017**, *61*, 94-103.

(7) Arshad, M. W.; Fosbøl, P. L. Von Solms, N.; Svendsen, H. F.; Thomsen, K., Heat of absorption of CO_2 in phase change solvents: 2-(diethylamino)ethanol and 3-(methylamino)propylamine. *J. Chem. Eng. Data* **2013**, *58* (7), 1974-1988.

(8) Hartono, A.; Saleem, F.; Arshad, M. W.; Usman, M.; Svendsen, H. F. Binary and ternary VLE of the 2-(diethylamino)-ethanol (DEEA)/3-(methylamino)-propylamine (MAPA)/water system. *Chem. Eng. Sci.* **2013**, *101* (0), 401-411.

(9) Garcia, M.; Knuutila, H. K.; Gu, S. Determination of Kinetics of CO_2 Absorption in Unloaded and Loaded DEEA+MAPA Blend. *Energy Procedia* **2017**, *114*, 1772-1784.

(10) Zhang, R.; Luo, X.; Yang, Q.; Yu, H.; Puxty, G.; Liang, Z. Analysis for the speciation in CO_2 loaded aqueous MEDA and MAPA solution using ^{13}C NMR technology. *Int. J. Greenhouse Gas Control* **2018**, *71*, 1-8.

(11) Perinu, C.; Bernhardsen, I. M.; Pinto, D. D. D.; Knuutila, H. K.; Jens, K.-J. NMR Speciation of Aqueous MAPA, Tertiary Amines, and Their Blends in the Presence of CO_2: Influence of pKa and Reaction Mechanisms. *Ind. Eng. Chem. Res.* **2018**, *57* (5), 1337-1349.

(12) Bernhardsen, I. M.; Krokvik, I. R. T.; Perinu, C.; Pinto, D. D. D.; Jens, K. J.; Knuutila, H. K. Influence of pKa on solvent performance of MAPA promoted tertiary amines. *Int. J. Greenhouse Gas Control* **2018**, *68*, 68-76.

(13) Liu, S.; Gao, H.; He, C.; Liang, Z. Experimental evaluation of highly efficient primary and secondary amines with lower energy by a novel method for post-combustion CO_2 capture. *Appl. Energy* **2019**, *233-234*, 443-452.

(14) Perinu, C.; Arstad, B.; Bouzga, A. M.; Jens, K.-J. ^{13}C and ^{15}N NMR Characterization of Amine Reactivity and Solvent Effects in CO_2 Capture. *J. Phys. Chem. B* **2014**, *118* (34), 10167-10174.

(15) Arstad, B.; Blom, R.; Swang, O. CO_2 Absorption in Aqueous Solutions of Alkanolamines: Mechanistic Insight from Quantum Chemical Calculations. *J. Phys. Chem. A* **2007**, *111* (7), 1222-1228.

(16) McCann, N.; Phan, D.; Wang, X.; Conway, W.; Burns, R.; Attalla, M.; Puxty, G.; Maeder, M. Kinetics and Mechanism of Carbamate Formation from $CO_{2(aq)}$, Carbonate Species, and Monoethanolamine in Aqueous Solution. *J. Phys. Chem. A* **2009**, *113* (17), 5022-5029.

(17) Versteeg, G. F.; Van Dijck, L. A. J.; Van Swaaij, W. P. M. On the kinetics between CO_2 and alkanolamines both in aqueous and non-auqoeus solutions. An overview. *Chem. Eng. Commun.* **1996**, *144* (1), 113-158.

(18) Crooks, J. E.; Donnellan, J. P. Kinetics and mechanism of the reaction between carbon dioxide and amines in aqueous solution. *J. Chem. Soc., Perkin Trans. 2* **1989**, (4), 331-333.

(19) Dell'Amico, D. B.; Calderazzo, F.; Labella, L.; Marchetti, F.; Pampaloni, G. Converting Carbon Dioxide into Carbamato Derivatives. *Chem. Rev.* **2003**, *103* (10), 3857-3898.

(20) Jørgensen, E.; Faurholt, C. Reactions between Carbon Dioxide and Amino Alcohols. *Acta Chem. Scand.* **1954**, *8*, 1141-1144.

(21) Behrens, R.; von Harbou, E.; Thiel, W. R.; Böttinger, W.; Ingram, T.; Sieder, G.; Hasse, H. Monoalkylcarbonate Formation in Methyldiethanolamine–H_2O–CO_2. *J. Ind. Eng. Chem.* **2017**, *56* (31), 9006-9015.

(22) Vaidya, P. D.; Kenig, E. Y. CO_2-Alkanolamine Reaction Kinetics: A Review of Recent Studies. *Chem. Eng. Technol.* **2007**, *30*, 1467-1474.

(23) Nitta, M.; Hayashi, K.; Furukawa, Y.; Sato, H.; Yamanaka, Y. ^{13}C-NMR Study of Acid Dissociation Constant (pKa) Effects on the CO_2 Absorption and Regeneration of Aqueous Tertiary Alkanolamine−Piperazine Blends. *Energy Procedia* **2014**, *63*, 1863-1868.

(24) Danckwerts, P. V. *Gas-Liquid reactions*. McGraw-Hill Book Co: New York, 1970.

(25) Lívanský, K. Effect of temperature and pH on absorption of carbon dioxide by a free level of mixed solutions of some buffers. *Folia Microbiol.* **1982**, *27* (1), 55-59.

(26) Kern, D. M. The hydration of carbon dioxide. *J. Chem. Educ.* **1960**, *37* (1), 14.

(27) Roughton, F. J.; Booth, V. H. The catalytic effect of buffers on the reaction $CO_2 + H_2O \leftrightarrows H_2CO_3$. *Biochem. J.* **1938**, *32* (11), 2049-2069.

(28) Yu, W.-C.; Astarita, G.; Savage, D. W. Kinetics of carbon dioxide absorption in solutions of methyldiethanolamine. *Chem. Eng. Sci.* **1985**, *40* (8), 1585-1590.

(29) Couchaux, G.; Barth, D.; Jacquin, M.; Faraj, A.; Grandjean, J. Kinetics of Carbon Dioxide with Amines. I. Stopped-Flow Studies in Aqueous Solutions. A Review. *Oil Gas Sci. Technol. – Rev. IFP Energies nouvelles* **2014**, *69* (5), 865-884.

(30) Blauwhoff, P. M. M.; Versteeg, G. F.; Van Swaaij, W. P. M. A study on the reaction between CO_2 and alkanolamines in aqueous solutions. *Chem. Eng. Sci.* **1983**, *38* (9), 1411-1429.

(31) Donaldson, T. L.; Nguyen, Y. N. Carbon Dioxide Reaction Kinetics and Transport in Aqueous Amine Membranes. *Ind. Eng. Chem. Fundam.* **1980**, *19* (3), 260-266.

(32) Liu, S.; Gao, H.; Luo, X.; Liang, Z. Kinetics and new mechanism study of CO_2 absorption into water and tertiary amine solutions by stopped-Flow technique. *AIChE J.* **2019**, *65* (2), 652-661.

(33) Caplow, M. Kinetics of carbamate formation and breakdown. *J. Am. Chem. Soc.* **1968**, *90*, 6795-6803.

(34) Lv, B.; Guo, B.; Zhou, Z.; Jing, G. Mechanisms of CO_2 Capture into Monoethanolamine Solution with Different CO_2 Loading during the Absorption/Desorption Processes. *Environ. Sci. Technol.* **2015**, *49* (17), 10728-10735.

(35) Svendsen, H. F.; Hessen, E. T.; Mejdell, T. Carbon dioxide capture by absorption, challenges and possibilities. *Chem. Eng. J.* **2011**, *171* (3), 718-724.

(36) Pinto, D. D. D.; Monteiro, J. G. M. S.; Johnsen, B.; Svendsen, H. F.; Knuutila, H. Density measurements and modelling of loaded and unloaded aqueous solutions of MDEA (N-methyldiethanolamine), DMEA (N,N-dimethylethanolamine), DEEA (diethylethanolamine) and MAPA (N-methyl-1,3-diaminopropane). *Int. J. Greenhouse Gas Control* **2014**, *25*, 173-185.

(37) Ma'mun, S.; Jakobsen, J. P.; Svendsen, H. F.; Juliussen, O. Experimental and Modeling Study of the Solubility of Carbon Dioxide in Aqueous 30 Mass % 2-((2-Aminoethyl)amino)ethanol Solution. *Ind. Eng. Chem. Res.* **2006**, *45* (8), 2505-2512.

(38) Perinu, C.; Arstad, B.; Jens, K.-J. NMR spectroscopy applied to amine–CO_2–H_2O systems relevant for post-combustion CO_2 capture: A review. *Int. J. Greenhouse Gas Control* **2014**, *20*, 230-243.

(39) Perinu, C.; Arstad, B.; Bouzga, A. M.; Svendsen, J. A.; Jens, K. J. NMR-Based Carbamate Decomposition Constants of Linear Primary Alkanolamines for CO_2 Capture. *Ind. Eng. Chem. Res.* **2014**, *53* (38), 14571-14578.

(40) Kim, I.; Svendsen, H. F. Heat of Absorption of Carbon Dioxide (CO_2) in Monoethanolamine (MEA) and 2-(Aminoethyl)ethanolamine (AEEA) Solutions. *Ind. Eng. Chem. Res.* **2007**, *46* (17), 5803-5809.

(41) Kim, I.; Hoff, K. A.; Mejdell, T. Heat of Absorption of CO_2 with Aqueous Solutions of MEA: New Experimental Data. *Energy Procedia* **2014**, *63*, 1446-1455.

(42) Kim, I. Heat of reaction and VLE of post combustion CO_2 absorbents. *PhD dissertation, Department of Chemical Engineering, Norwegian University of Science and Technology, Trondheim.* **2009**.

(43) Kim, I.; Svendsen, H. F. Comparative study of the heats of absorption of post-combustion CO_2 absorbents. *Int. J. Greenhouse Gas Control* **2011**, *5* (3), 390-395.

(44) Ciftja, A. F.; Hartono, A.; Svendsen, H. F. Experimental study on phase change solvents in CO_2 capture by NMR spectroscopy. *Chem. Eng. Sci.* **2013**, *102*, 378-386.

(45) Perinu, C.; Bernhardsen, I. M.; Svendsen, H. F.; Jens, K.-J. CO_2 Capture by Aqueous 3-(Methylamino)propylamine in Blend with Tertiary Amines: An NMR Analysis. *Energy Procedia* **2017**, *114*, 1949-1955.

(46) Kortunov, P. V.; Siskin, M.; Paccagnini, M.; Thomann, H. CO_2 Reaction Mechanisms with Hindered Alkanolamines: Control and Promotion of Reaction Pathways. *Energy Fuels* **2016**, 30 (2), 1223-1236

(47) Rayer, A. V.; Henni, A. Heats of Absorption of CO_2 in Aqueous Solutions of Tertiary Amines: N-Methyldiethanolamine, 3-Dimethylamino-1-propanol, and 1-Dimethylamino-2-propanol. *Ind. Eng. Chem. Res.* **2014**, *53* (12), 4953-4965.

(48) Jiang, W.; Luo, X.; Gao, H.; Liang, Z.; Liu, B.; Tontiwachwuthikul, P.; Hu, X. A comparative kinetics study of CO_2 absorption into aqueous DEEA/MEA and DMEA/MEA blended solutions. *AIChE J.* **2018**, *64* (4), 1350-1358.

Graph for the table of contents only
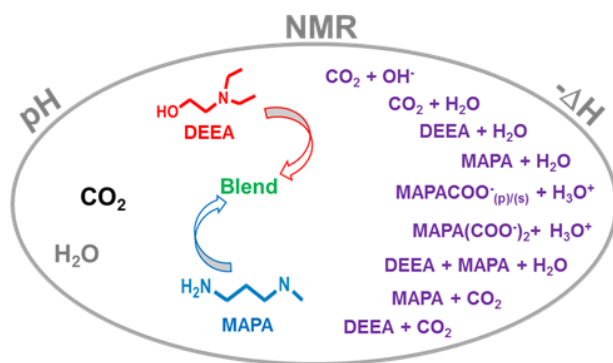
Supporting Information

Aqueous MAPA, DEEA and their blend as CO$_2$ absorbents: Interrelationship between NMR speciation, pH and heat of absorption

Cristina Perinu,[1] Ida M. Bernhardsen,[2] Diego D.D. Pinto,[2] Hanna K. Knuutila,[2]

Klaus J. Jens.*[1]

[1]Department of Process, Energy and Environmental Technology, University of Southeast Norway, Postbox 235, NO-3603 Kongsberg, Norway

[2]Department of Chemical Engineering, Norwegian University of Science and Technology (NTNU), NO-7491 Trondheim, Norway

* klaus.j.jens@usn.no

Table S1: Density, as measured by Anton Paar DMA 4500 M densitometer, of aqueous MAPA 1M, DEEA 3M and MAPA 1M-DEEA 3M before addition of CO_2.

	density (g/ml)
MAPA 1M - DEEA 3M	0.97572
MAPA 1M	0.99094
DEEA 3M	0.98334

Table S2. Weight of 1 mL of each CO_2 loaded sample.

MAPA 1M - DEEA 3M										
mol_{CO2}/mol_{amine}	0.05	0.11	0.17	0.22	0.34	0.47	0.59	0.72	0.85	0.96
density (g in 1ml)	0.9797	0.9851	0.999	1.0132	1.026	1.049	1.0685	1.084	1.102	1.1121
MAPA 1M										
mol_{CO2}/mol_{amine}	0.11	0.20	0.27	0.36	0.54	0.75	0.94	1.12	1.25	1.50
density (g in 1ml)	0.9866	0.9908	1.0056	1.0061	1.005	1.0201	1.0268	1.0247	1.0359	1.0444
DEEA 3M										
mol_{CO2}/mol_{amine}	0.04	0.10	0.14	0.19	0.28	0.39	0.47	0.59	0.69	0.93
density (g in 1ml)	0.9881	0.9879	1.0026	1.0016	1.0209	1.0312	1.0462	1.055	1.0633	1.0846

Table S3. pH measured in each sample.

MAPA1M- DEEA 3M											
mol_{CO2}/mol_{amine}	0.00	0.05	0.11	0.16	0.22	0.34	0.45	0.58	0.72	0.86	0.97
pH	12.78	11.44	11.13	10.87	10.66	10.28	10.02	9.8	9.53	9.13	8.53
MAPA 1M											
mol_{CO2}/mol_{amine}	0.00	0.10	0.18	0.27	0.38	0.57	0.76	0.95	1.17	1.36	1.47
pH	12.4	11.66	11.3	11.12	10.97	10.58	10.23	9.53	8.45	7.9	7.77
DEEA 3M											
mol_{CO2}/mol_{amine}	0.00	0.05	0.09	0.14	0.18	0.27	0.37	0.47	0.56	0.67	0.98
pH	12.07	10.79	10.53	10.38	10.27	10.11	10.01	9.82	9.67	9.57	8.41

Table S4. Differential heat of absorption of CO_2 in aqueous MAPA 1M at 25°C.

mol$_{CO2}$/mol$_{amine}$	-ΔH (kJ/mol$_{CO2}$)
0.11	100.205
0.28	100.458
0.45	96.224
0.62	96.670
0.84	94.611
1.03	65.527
1.23	42.289
1.41	42.655
1.58	40.320
1.74	35.798
1.83	29.562

Table S5. Differential heat of absorption of CO_2 in aqueous MAPA 1M at 40°C.

mol$_{CO2}$/mol$_{amine}$	-ΔH (kJ/mol$_{CO2}$)
0.21	98.2799
0.43	94.2602
0.65	93.6375
0.87	88.0429
1.08	63.7486
1.27	43.9388
1.46	36.7198
1.70	35.1281

Table S6. Differential heat of absorption of CO_2 in aqueous DEEA 3M at 25°C.

mol$_{CO2}$/mol $_{amine}$	-ΔH (kJ/mol$_{CO2}$)
0.06	81.33
0.11	73.51
0.25	72.23
0.39	67.74
0.53	62.99
0.67	63.32
0.80	54.02
0.88	49.09
0.98	35.38
1.00	19.61

Table S7. Differential heat of absorption of CO_2 in aqueous DEEA 3M at 40°C.

mol$_{CO2}$/mol $_{amine}$	-ΔH (kJ/mol$_{CO2}$)
0.06	78.99
0.12	73.38
0.23	70.02
0.34	67.54
0.44	65.37
0.56	60.14
0.72	57.31
0.88	51.35
0.98	37.01

Table S8. Differential heat of absorption of CO_2 in aqueous MAPA 1M-DEEA 3M at 25°C.

mol$_{CO2}$/mol$_{amine}$	-ΔH (kJ/mol$_{CO2}$)
0.07	103.60
0.14	95.41
0.21	95.35
0.28	93.04
0.35	87.53
0.41	83.73
0.48	78.48
0.55	74.49
0.62	67.55
0.69	63.65
0.76	59.52
0.83	54.78
0.96	49.11
1.05	40.88

Table S9. Concentration (mol/L) of each species in aqueous MAPA 1M-CO_2 systems.

mol$_{CO2}$/mol$_{amine}$	0.11	0.20	0.27	0.36	0.54	0.75	0.94	1.12	1.25	1.50
MAPACOO$^-$$_{(p)}$	0.062	0.121	0.173	0.235	0.336	0.472	0.604	0.625	0.566	0.419
MAPA(COO$^-$)$_2$		0.000	0.006	0.009	0.020	0.032	0.032	0.021		
MAPACOO$^-$$_{(s)}$	0.016	0.034	0.045	0.061	0.084	0.109	0.134	0.135	0.124	0.089
MAPA	0.894	0.806	0.748	0.680	0.489	0.346	0.219	0.176	0.281	0.421
HCO$_3$$^-$/CO$_3$$^{2-}$	0.022	0.035	0.044	0.055	0.066	0.078		0.239	0.513	0.841

Table S10. Concentration (mol/L) of each species in aqueous DEEA 3M-CO$_2$ systems.

mol$_{CO2}$/mol$_{amine}$	0.04	0.10	0.14	0.19	0.28	0.39	0.47	0.59	0.69	0.93
DEEA	2.806	2.999	2.979	3.261	2.893	3.023	3.163	2.963	3.018	2.991
DEEAOCOO$^-$	0.01	0.02	0.023	0.021	0.043	0.057	0.072	0.078	0.087	0.108
HCO$_3^-$/CO$_3^{2-}$	0.123	0.279	0.417	0.575	0.797	1.012	1.459	1.820	2.110	2.912

Table S11. Concentration (mol/L) of each species in aqueous MAPA1M-DEEA3M-CO$_2$ systems

mol$_{CO2}$/mol$_{amine}$	0.05	0.11	0.17	0.22	0.34	0.47	0.59	0.72	0.85	0.96
MAPACOO$^-_{(p)}$	0.152	0.328	0.398	0.472	0.524	0.489	0.484	0.514	0.563	0.621
MAPA(COO$^-$)$_2$	0.007	0.028	0.054	0.092	0.248	0.395	0.444	0.428	0.269	0.143
MAPACOO$^-_{(s)}$	0.046	0.095	0.121	0.143	0.147	0.134	0.128	0.129	0.135	0.146
MAPA	0.795	0.621	0.392	0.246	0.074	0.032	0.023	0.021	0.028	0.059
HCO$_3^-$/CO$_3^{2-}$			0.041	0.057	0.193	0.531	1.056	1.604	2.138	2.549
DEEA	3.063	3.255	2.956	2.888	3.023	3.163	3.230	3.173	2.897	2.769
DEEAOCOO$^-$			0.000	0.000	0.000	0.034	0.059	0.073	0.084	0.092

Table S12. Chemical shift values of the signal corresponding to HCO$_3^-$/CO$_3^{2-}$ in the ^{13}C NMR spectra of aqueous MAPA 1M, DEEA 3M and MAPA 1M – DEEA 3M at increasing addition of CO$_2$ into the solution.

	mol$_{CO2}$/mol$_{amine}$	0.11	0.2	0.27	0.36	0.54	0.75	0.94	1.12	1.25	1.5
MAPA 1M	δ (ppm) HCO$_3^-$/CO$_3^{2-}$	168.2	168.1	167.8	167.8	167.3	166.4		161.9	161.1	161
	mol$_{CO2}$/mol$_{amine}$	0.04	0.1	0.14	0.19	0.28	0.39	0.47	0.59	0.69	0.93
DEEA 3M	δ (ppm) HCO$_3^-$/CO$_3^{2-}$	165.7	165.2	164.8	164.5	164.1	163.7	163.3	162.8	162.3	161.3
	mol$_{CO2}$/mol$_{amine}$	0.05	0.11	0.17	0.22	0.34	0.47	0.59	0.72	0.85	0.96
MAPA1M-DEEA 3M	δ (ppm) HCO$_3^-$/CO$_3^{2-}$			165.7	165.1	163.9	163	162.4	161.9	161.4	161.2
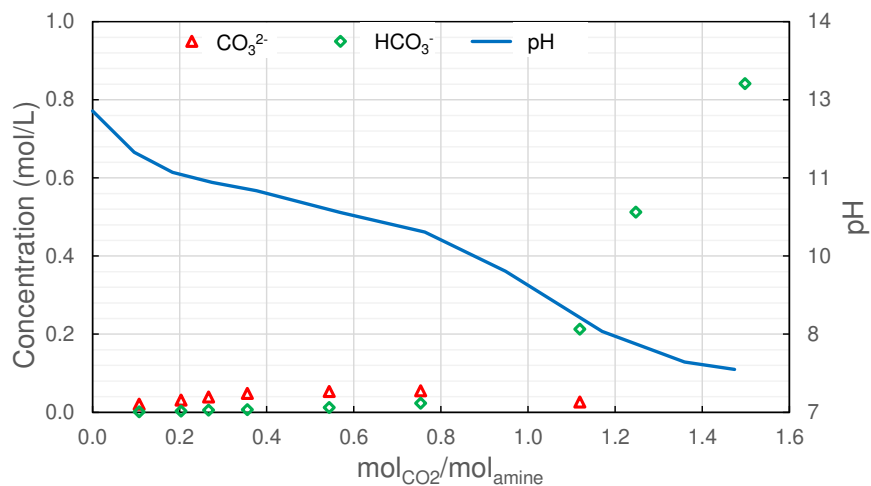
Figure S1. Estimation of the HCO_3^- and CO_3^{2-} content in MAPA 1M-CO_2-H_2O systems. Calculation based on the calibration curve developed in Perinu et al. 2014.[1]
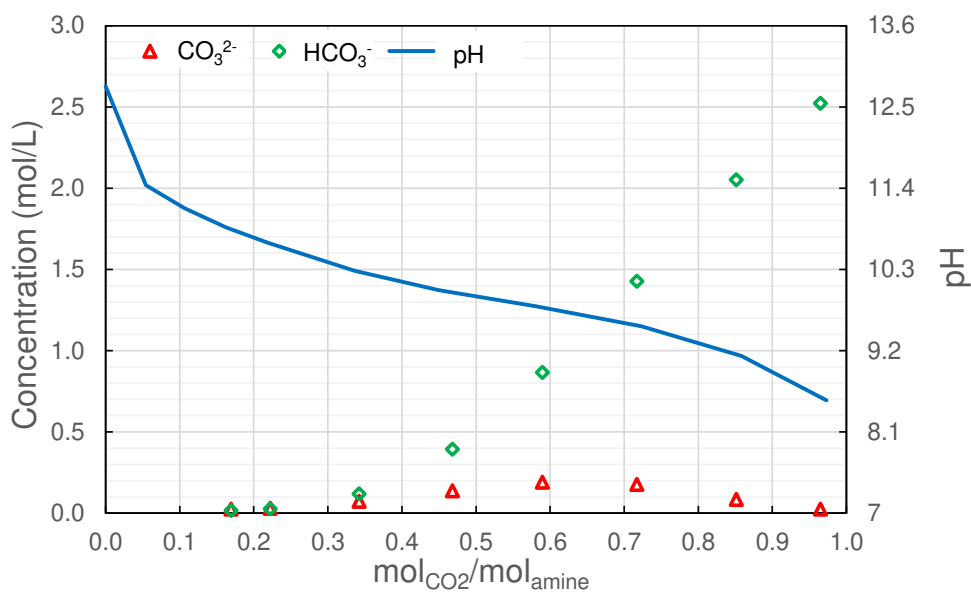
Figure S2. Estimation of the HCO_3^- and CO_3^{2-} content in MAPA 1M-DEEA 3M-CO_2-H_2O systems. Calculation based on the calibration curve developed in Perinu et al. 2014.[1]

References

1.   Perinu, C.; Arstad, B.; Bouzga, A. M.; Svendsen, J. A.; Jens, K. J., NMR-Based Carbamate Decomposition Constants of Linear Primary Alkanolamines for CO2 Capture. *Industrial & Engineering Chemistry Research* **2014,** 53, (38), 14571-14578.